Synthesis of Monodisperse Mesoporous Titania Beads with Controllable Diameter, High Surface Areas, and Variable Pore Diameters (14−23 nm)

ARTICLE *in* JOURNAL OF THE AMERICAN CHEMICAL SOCIETY · MARCH 2010

Impact Factor: 12.11 · DOI: 10.1021/ja100040p · Source: PubMed

J|A|C|S ARTICLES

Published on Web 03/04/2010

Synthesis of Monodisperse Mesoporous Titania Beads with Controllable Diameter, High Surface Areas, and Variable Pore Diameters (14−23 nm)

Dehong Chen,[†] Lu Cao,[†] Fuzhi Huang,[‡] Paolo Imperia,[§] Yi-Bing Cheng,*[,‡] and Rachel A. Caruso*[,†,||]

PFPC, School of Chemistry, The University of Melbourne, Melbourne, Victoria 3010, CSIRO Materials Science and Engineering, Private Bag 33, Clayton South, Victoria 3169, Department of Materials Engineering, Monash University, Melbourne, Victoria 3800, and The Bragg Institute and Institute of Materials Engineering, ANSTO, Lucas Heights, New South Wales 2234, Australia

Received January 4, 2010; E-mail: yibing.cheng@eng.monash.edu.au; rcaruso@unimelb.edu.au

Abstract: Monodisperse mesoporous anatase titania beads with high surface areas and tunable pore size and grain diameter have been prepared through a combined sol−gel and solvothermal process in the presence of hexadecylamine (HDA) as a structure-directing agent. The monodispersity of the resultant titania beads, along with the spherical shape, can be controlled by varying the amount of structure-directing agent involved in the sol−gel process. The diameter of the titania beads is tunable from ∼320 to 1150 nm by altering the hydrolysis and condensation rates of the titanium alkoxide. The crystallite size, specific surface area (from 89 to 120 m^2/g), and pore size distribution (from 14 to 23 nm) of the resultant materials can be varied through a mild solvothermal treatment in the presence of varied amounts of ammonia. On the basis of the results of small-angle XRD, high-resolution SEM/TEM, and gas sorption characterization, a mechanism for the formation of the monodisperse precursor beads has been proposed to illustrate the role of HDA in determining the morphology and monodispersity during the sol−gel synthesis. The approach presented in this study demonstrates that simultaneous control of the physical properties, including specific surface area, mesoporosity, crystallinity, morphology, and monodispersity, of the titania materials can be achieved by a facile sol−gel synthesis and solvothermal process.

Introduction

Owing to its specific functional characteristics and importance in a wide variety of technical fields, titania has been investigated intensively in various research areas including inorganic pigment, sunscreen, photocatalysis, energy storage and conversion, electrochromics, and sensor fields.[1−4] The effectiveness of titania in practical applications varied considerably with its specific surface area and mesoporosity,[5,6] composition,[7−9] crystallinity[10,11] and, importantly, the morphology and texture of the material.[10−17] The controlled synthesis of titania materials with well-defined structural architectures, such as single crystals,[17−24] ordered mesoporous thin films,[25−27] nanotubes,[16,28,29] porous networks,[30−33]

[†] The University of Melbourne.
[‡] Monash University.
[§] ANSTO.
[||] CSIRO Materials Science and Engineering.

(1) Grätzel, M. *Nature* **2001**, *414*, 338.
(2) Wijnhoven, J.; Vos, W. L. *Science* **1998**, *281*, 802.
(3) Chen, X.; Mao, S. S. *Chem. Rev.* **2007**, *107*, 2891.
(4) Fujishima, A.; Zhang, X. T.; Tryk, D. A. *Surf. Sci. Rep.* **2008**, *63*, 515.
(5) Yang, P. D.; Zhao, D. Y.; Margolese, D. I.; Chmelka, B. F.; Stucky, G. D. *Nature* **1998**, *396*, 152.
(6) Tian, B. Z.; Liu, X. Y.; Tu, B.; Yu, C. Z.; Fan, J.; Wang, L. M.; Xie, S. H.; Stucky, G. D.; Zhao, D. Y. *Nat. Mater.* **2003**, *2*, 159.
(7) Enache, D. I.; Edwards, J. K.; Landon, P.; Solsona-Espriu, B.; Carley, A. F.; Herzing, A. A.; Watanabe, M.; Kiely, C. J.; Knight, D. W.; Hutchings, G. J. *Science* **2006**, *311*, 362.
(8) Dong, W. Y.; Sun, Y. J.; Lee, C. W.; Hua, W. M.; Lu, X. C.; Shi, Y. F.; Zhang, S. C.; Chen, J. M.; Zhao, D. Y. *J. Am. Chem. Soc.* **2007**, *129*, 13894.
(9) Wang, X. H.; Li, J. G.; Kamiyama, H.; Katada, M.; Ohashi, N.; Moriyoshi, Y.; Ishigaki, T. *J. Am. Chem. Soc.* **2005**, *127*, 10982.
(10) Lee, J.; Orilall, M. C.; Warren, S. C.; Kamperman, M.; Disalvo, F. J.; Wiesner, U. *Nat. Mater.* **2008**, *7*, 222.
(11) Testino, A.; Bellobono, I. R.; Buscaglia, V.; Canevali, C.; D'Arienzo, M.; Polizzi, S.; Scotti, R.; Morazzoni, F. *J. Am. Chem. Soc.* **2007**, *129*, 3564.
(12) Matthey, D.; Wang, J. G.; Wendt, S.; Matthiesen, J.; Schaub, R.; Laegsgaard, E.; Hammer, B.; Besenbacher, F. *Science* **2007**, *315*, 1692.
(13) Wang, K. X.; Wei, M. D.; Morris, M. A.; Zhou, H. S.; Holmes, J. D. *Adv. Mater.* **2007**, *19*, 3016.
(14) Zhou, H. S.; Li, D. L.; Hibino, M.; Honma, I. *Angew. Chem., Int. Ed.* **2005**, *44*, 797.
(15) Zukalova, M.; Zukal, A.; Kavan, L.; Nazeeruddin, M. K.; Liska, P.; Grätzel, M. *Nano Lett.* **2005**, *5*, 1789.
(16) Varghese, O. K.; Paulose, M.; Grimes, C. A. *Nat. Nanotechnol.* **2009**, *4*, 592.
(17) Yang, H. G.; Sun, C. H.; Qiao, S. Z.; Zou, J.; Liu, G.; Smith, S. C.; Cheng, H. M.; Lu, G. Q. *Nature* **2008**, *453*, 638.
(18) Amano, F.; Prieto-Mahaney, O. O.; Terada, Y.; Yasumoto, T.; Shibayama, T.; Ohtani, B. *Chem. Mater.* **2009**, *21*, 2601.
(19) Dai, Y. Q.; Cobley, C. M.; Zeng, J.; Sun, Y. M.; Xia, Y. N. *Nano Lett.* **2009**, *9*, 2455.
(20) Han, X. G.; Kuang, Q.; Jin, M. S.; Xie, Z. X.; Zheng, L. S. *J. Am. Chem. Soc.* **2009**, *131*, 3152.
(21) Liu, G.; Yang, H. G.; Wang, X. W.; Cheng, L. N.; Pan, J.; Lu, G. Q.; Cheng, H. M. *J. Am. Chem. Soc.* **2009**, *131*, 12868.
(22) Yang, H. G.; Liu, G.; Qiao, S. Z.; Sun, C. H.; Jin, Y. G.; Smith, S. C.; Zou, J.; Cheng, H. M.; Lu, G. Q. *J. Am. Chem. Soc.* **2009**, *131*, 4078.

 10.1021/ja100040p

and spherical particles,[34−45] has drawn a lot of attention in recent years. For example, anatase single crystals containing a high percentage of reactive facets have been synthesized via a hydrothermal process in the presence of fluorine species.[17,20–24] Thermally stable mesoporous titania thin films with uniform pores can be prepared through an evaporation-induced self-assembly method in the presence of various block copolymers.[25–27] Titania nanotubes having different aspect ratios can be fabricated via anodization of titanium foil with variable potential and electrolyte composition.[16,28,29] Through a sol−gel nanocasting process, three-dimensional interconnected titania networks with high crystallinity and controllable macropores have been successfully replicated from preformed templates.[31–33]

Among the various morphologies and textures of the reported titania materials, the spherical titania particles have shown highly promising applications in the energy and environment-related fields.[34–45] The spherical titania particles with hollow, chestnut-like, and finely tunable configurations have been synthesized using different strategies including the hydrothermal method, templating synthesis, and a modified sol−gel process.[34–45] However, the simultaneous demands of maintaining the required properties (including high surface area, large mesopores, and high crystallinity) as well as the sphericity make the preparation of such mesoporous anatase titania materials a challenge among the materials community. To our knowledge, a facile process has not been developed to obtain titania materials with all of the above features, mainly due to the extremely high reactivity of the titanium dioxide precursors and the complexity of the synthetic procedures.

In this paper, we report the synthesis of monodisperse mesoporous anatase titania beads with high surface area and tunable pore size and grain diameter via a combined sol−gel and solvothermal process in the presence of hexadecylamine (HDA) as a structure-directing agent. The morphology, monodispersity, and bead diameter (from ∼320 to 1150 nm) of the resultant materials can be controlled via a cooperative self-assembly process in the sol−gel synthesis, while the crystallite size, specific surface area, and pore size distribution of the titania beads can be varied by altering the ammonia concentration in a mild solvothermal process. The role of HDA in determining the morphology and monodispersity of the precursor beads during the sol−gel synthesis has been illustrated in a proposed mechanism of formation. The integrated features of the beads, including high specific surface area, large pore size, high crystallinity, and well-defined morphology, would make such materials excellent candidates for applications in areas of energy conversion and environmental cleanup.

Experimental Section

Chemicals. Titanium(IV) isopropoxide (TIP; 97%) and HDA (90%) were purchased from Sigma-Aldrich. Absolute ethanol (>99.7%, Merck), potassium chloride (AR, BDH), ammonia solution (25%, BDH), and Milli-Q water (18.2 MΩ cm) were used for the synthesis.

Preparation. The amorphous precursor beads were prepared via a sol−gel process in the presence of HDA as a structure-directing agent. KCl was used to control the monodispersity of the precursor beads by adjusting the ionic strength of the solution.[46] The solution composition of HDA:H_2O:KCl:ethanol:TIP (molar ratio) was varied in the range of (0−1.0):(1−10):5.5×10^{-3}:236.5:1.0. In a typical synthesis, 7.95 g of HDA was dissolved in 800 mL of ethanol, followed by the addition of 3.20 mL of KCl solution (0.1 M). To this solution was added 18.10 mL of TIP under vigorous stirring at ambient temperature. The milky white precursor bead suspension was kept static for 18 h and then centrifuged, and the beads were washed with ethanol three times and dried in air at room temperature. The precursor bead samples were labeled with PB- as a prefix followed by the HDA:Ti molar ratio (xHDA) and the H_2O:Ti molar ratio ($y$$H_2O$) in the general form of PB-xHDA-$y$$H_2O$. For instance, PB-0.50HDA-3H_2O refers to the precursor bead sample prepared with an HDA:Ti molar ratio of 0.50 and H_2O:Ti = 3. A portion of the samples was directly calcined, denoted as PB-xHDA-$y$$H_2O$-calcined.

To prepare mesoporous titania beads with a highly crystalline framework, a solvothermal treatment of the precursor beads was performed. A 1.6 g of the amorphous precursor beads was dispersed in a 20 mL ethanol and 10 mL Milli-Q water mixture with an ammonia concentration of 0, 0.22, and 0.45 M. Then the resulting mixtures were sealed within a Teflon-lined autoclave (50 mL) and heated at 160 °C for 16 h. After filtration and ethanol washing, the air-dried powders were calcined at 500 °C for 2 h in air to remove organic components and produce the mesoporous TiO_2 beads for characterization. Such calcined materials were denoted as TiO_2-xHDA-$y$$H_2O$-$z$M, where x = HDA:Ti molar ratio, y = H_2O:Ti molar ratio, and z = ammonia concentration for the solvothermal treatment.

Characterization. Powder X-ray diffraction (XRD; Philips PW1800 diffractometer) was used to determine the crystalline phase and estimate the crystal size of the resulting titania beads. The morphologies of the samples were observed by using a high-resolution field emission environmental scanning electron microscope (Quanta 200 FEI) without sputter coating pretreatment. TEM images and selected area electron diffraction (SAED) patterns of the resulting titania beads were obtained on an FEI Tecnai F20 transmission electron microscope operating at 200 kV. To investigate the interior structures of the resulting mesoporous titania beads, the samples were embedded in an LR-white resin and

(23) Zhang, D. Q.; Li, G. S.; Yang, X. F.; Yu, J. C. *Chem. Commun.* **2009**, 4381.
(24) Alivov, Y.; Fan, Z. Y. *J. Phys. Chem. C* **2009**, *113*, 12954.
(25) Choi, S. Y.; Mamak, M.; Coombs, N.; Chopra, N.; Ozin, G. A. *Adv. Funct. Mater.* **2004**, *14*, 335.
(26) Li, D. L.; Zhou, H. S.; Honma, I. *Nat. Mater.* **2004**, *3*, 65.
(27) Crepaldi, E. L.; Soler-Illia, G.; Grosso, D.; Cagnol, F.; Ribot, F.; Sanchez, C. *J. Am. Chem. Soc.* **2003**, *125*, 9770.
(28) Shankar, K.; Bandara, J.; Paulose, M.; Wietasch, H.; Varghese, O. K.; Mor, G. K.; LaTempa, T. J.; Thelakkat, M.; Grimes, C. A. *Nano Lett.* **2008**, *8*, 1654.
(29) Zhu, K.; Neale, N. R.; Miedaner, A.; Frank, A. J. *Nano Lett.* **2007**, *7*, 69.
(30) Shchukin, D. G.; Caruso, R. A. *Adv. Funct. Mater.* **2003**, *13*, 789.
(31) Caruso, R. A.; Antonietti, M.; Giersig, M.; Hentze, H. P.; Jia, J. G. *Chem. Mater.* **2001**, *13*, 1114.
(32) Caruso, R. A.; Schattka, J. H. *Adv. Mater.* **2000**, *12*, 1921.
(33) Zhou, J. F.; Zhou, M. F.; Caruso, R. A. *Langmuir* **2006**, *22*, 3332.
(34) Dong, A. G.; Ren, N.; Tang, Y.; Wang, Y. J.; Zhang, Y. H.; Hua, W. M.; Gao, Z. *J. Am. Chem. Soc.* **2003**, *125*, 4976.
(35) Meyer, U.; Larsson, A.; Hentze, H. P.; Caruso, R. A. *Adv. Mater.* **2002**, *14*, 1768.
(36) Chen, D. H.; Huang, F. Z.; Cheng, Y. B.; Caruso, R. A. *Adv. Mater.* **2009**, *21*, 2206.
(37) Guo, Y. G.; Hu, Y. S.; Maier, J. *Chem. Commun.* **2006**, 2783.
(38) Guo, Y. G.; Hu, Y. S.; Sigle, W.; Maier, J. *Adv. Mater.* **2007**, *19*, 2087.
(39) Yin, J. B.; Xiang, L. Q.; Zhao, X. P. *Appl. Phys. Lett.* **2007**, *90*, 113112.
(40) Chi, B.; Zhao, L.; Jin, T. *J. Phys. Chem. C* **2007**, *111*, 6189.
(41) Cho, C. H.; Kim, D. K.; Kim, D. H. *J. Am. Ceram. Soc.* **2003**, *86*, 1138.
(42) Deshpande, A. S.; Shchukin, D. G.; Ustinovich, E.; Antonietti, M.; Caruso, R. A. *Adv. Funct. Mater.* **2005**, *15*, 239.
(43) Li, H. X.; Bian, Z. F.; Zhu, J.; Zhang, D. Q.; Li, G. S.; Huo, Y. N.; Li, H.; Lu, Y. F. *J. Am. Chem. Soc.* **2007**, *129*, 8406.
(44) Shchukin, D. G.; Caruso, R. A. *Chem. Mater.* **2004**, *16*, 2287.
(45) Jiang, X. C.; Herricks, T.; Xia, Y. N. *Adv. Mater.* **2003**, *15*, 1205.
(46) Eiden-Assmann, S.; Widoniak, J.; Maret, G. *Chem. Mater.* **2004**, *16*, 6.

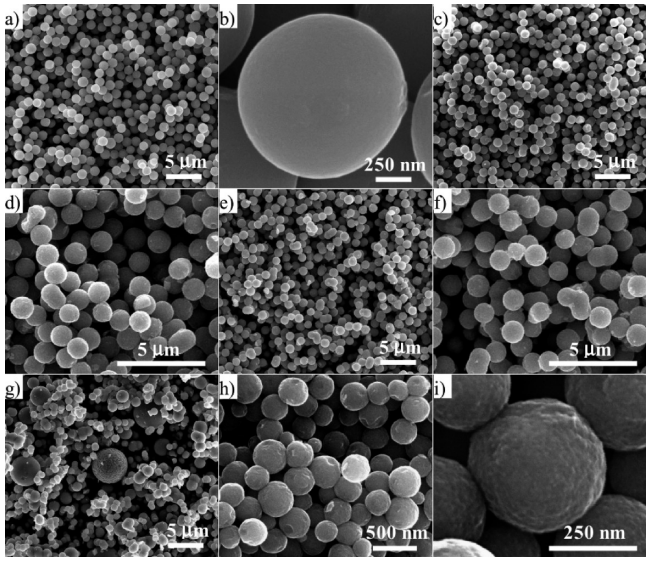

Figure 1. SEM images of the precursor materials synthesized with varying HDA:Ti molar ratio: (a, b) 1:1, (c, d) 0.25:1, (e, f) 0.10:1, (g) 0.05:1, (h, i) 0:1. The H_2O:Ti molar ratio was 3:1 for these materials. Note: all the images were obtained without sputter coating.

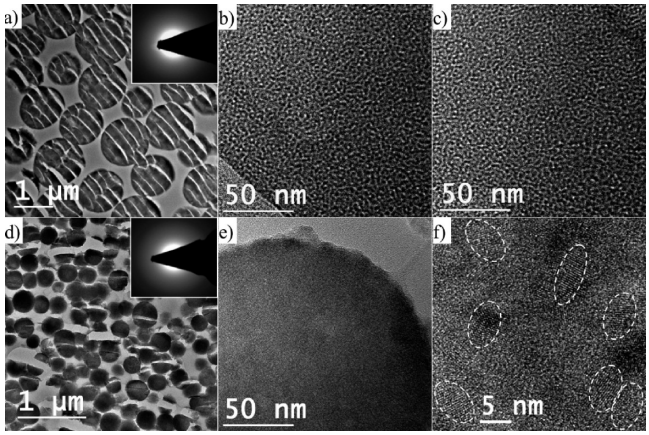

Figure 2. TEM images and SAED patterns of the ultramicrotomed sections of the precursor beads synthesized (a−c) with an HDA:Ti molar ratio of 1:1 and (d−f) without the HDA structure-directing agent. The H_2O:Ti molar ratio was 3:1 for these samples. The images in (b) and (c) show the edge and the core of a bead, respectively. The parallel ridgelines observed for the bead sections in (a) were a result of the ultramicrotoming during TEM sample preparation.

ultramicrotomed to 60 nm thick sections. Nitrogen sorption isotherms were measured at −196 °C by using a Micromeritics Tristar 3000 system. Prior to the measurement, the precursor beads were degassed at 50 °C and the calcined samples were degassed at 160 °C on a vacuum line, both for 18 h. The standard multipoint Brunauer−Emmett−Teller (BET) method was utilized to calculate the specific surface area using the adsorption data in the P/P_o range from 0.05 to 0.20. The pore size distributions of the materials were derived from the adsorption branches of the isotherms on the basis of the Barett−Joyner−Halenda (BJH) model.

Results and Discussion

Amorphous Precursor Beads. 1. Effect of the HDA:Ti Molar Ratio. The first step in the fabrication of mesoporous anatase titania beads is the sol−gel process. This involves adding TIP to an ethanol mixture containing the HDA structure-directing agent and KCl aqueous solution to instigate the hydrolysis and

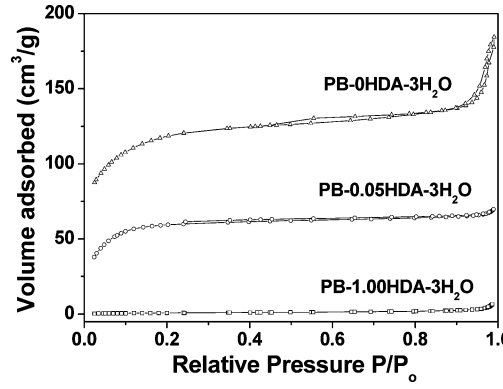

Figure 3. Nitrogen sorption isotherms of the precursor materials synthesized with varying HDA:Ti molar ratio. The H_2O:Ti molar ratio was 3:1 for these materials.

condensation reactions. Spherical beads can be produced after the sol−gel process over a range of synthesis conditions. The amount of HDA used influences the morphological characteristics of the precursor beads. Figure 1 shows SEM images of the precursor beads obtained with varying molar ratios of HDA to Ti. When the molar ratio is 1:1, the precursor beads are monodisperse, individual entities having smooth surfaces (Figure 1a,b). For the conditions studied here, the sphere diameter is 1150 ± 40 nm. The precursor beads remain relatively monodisperse when the HDA quantity is decreased to an HDA:Ti molar ratio of 0.25:1, while the occasional presence of dimers becomes apparent (Figure 1c,d), indicating merging of the spheres during formation. Dimers and trimers become more abundant as the HDA:Ti ratio further decreases (Figure 1e,f), finally producing polydisperse spheres when the HDA:Ti molar ratio is 0.05:1 (Figure 1g). When the synthesis is conducted without HDA, polydisperse beads form with diameters ranging from 150 to 400 nm (Figure 1h), and the sphere surfaces are roughly textured, indicating agglomeration of smaller subunits in the bead construction (Figure 1i). Hence, the presence of HDA during the sol−gel synthesis at HDA:Ti molar ratios of 0.25:1 or above afforded individual, monodisperse spheres with smooth surfaces.

The precursor beads synthesized with an HDA:Ti molar ratio of 1:1 are solid to the core (Figure 2a) and possess a homogeneous wormhole-like mesostructure (Figure 2b). This mesostructure is similar throughout the whole bead, from the surface to the core (Figure 2c). Such wormhole-like mesostructures were also confirmed by the small-angle XRD pattern shown in Figure SI-1 in the Supporting Information (SI). The corresponding SAED pattern confirms the amorphous nature of the precursor beads (Figure 2a inset), and this result is also supported by the wide-angle XRD pattern (see Figure SI-2, SI). In comparison, beads prepared without HDA present were also ultramicrotomed, and the TEM images are shown in Figure 2d. Again the spheres were not hollow in nature; however, no mesostructure was observed in these beads (Figure 2e), and no diffraction peak appeared in the corresponding small-angle XRD pattern for the sample (Figure SI-1, SI). Although both the SAED pattern (Figure 2d inset) and the wide-angle XRD analysis revealed that the beads prepared without HDA had an amorphous structure, the high-resolution TEM images (for example, Figure 2f) indicate the presence of crystal lattice fringes within the amorphous matrix of the beads that could be indexed to the (101) planes of anatase titania (see Figure SI-3, SI). The above differences indicate that the HDA plays an

Table 1. Physical Properties of the Amorphous Precursor Beads[a]

sample name	induction time (s)	diameter (nm)	S_{BET} (m^2/g)	V_{sp} (cm^3/g)
PB-1.00HDA-3H_2O	6 ± 1	1150 ± 40	3.05	0.008
PB-0.50HDA-3H_2O	7 ± 1	1150 ± 40	3.27	0.009
PB-0.33HDA-3H_2O	8 ± 1	1150 ± 40	3.02	0.008
PB-0.25HDA-3H_2O	12 ± 1	~1150 with dimers	3.24	0.009
PB-0.20HDA-3H_2O	16 ± 1	~1150 with dimers	3.29	0.009
PB-0.10HDA-3H_2O	31 ± 2	~1000 with dimers	3.79	0.009
PB-0.05HDA-3H_2O	58 ± 3	1000−5000	216	0.106
PB-0.02HDA-3H_2O	132 ± 3	1000−5000	405	0.189
PB-0.01HDA-3H_2O	175 ± 3	1000−5000	427	0.208
PB-0HDA-3H_2O	1034 ± 20	150−400	422	0.258
PB-0.50HDA-2H_2O	22 ± 2	1000−1550	3.26	0.010
PB-0.50HDA-3H_2O	7 ± 1	1150 ± 40	3.27	0.009
PB-0.50HDA-4H_2O	3 ± 0.5	730 ± 40	4.39	0.015
PB-0.50HDA-5H_2O	2 ± 0.5	640 ± 40	5.43	0.020
PB-0.50HDA-6H_2O	~1	500 ± 50	6.47	0.024
PB-0.50HDA-7H_2O	<1	420 ± 50	8.04	0.032
PB-0.50HDA-8H_2O	<1	~360 with dimers	8.66	0.034
PB-0.50HDA-10H_2O	<1	~320 with dimers	9.64	0.037

[a] Induction time refers to the period of time after adding TIP until the milky white solution formed. S_{BET} = BET specific surface area obtained from N_2 adsorption data in the P/P_o range from 0.05 to 0.20. V_{sp} = single-point pore volume calculated from the N_2 adsorption isotherm at $P/P_o = 0.98$.

important role in the formation of the wormhole-like mesostructure, a well-known structure present in the short-range ordered mesoporous silica fabricated in the presence of nonionic surfactants via a neutral templating route.[47,48]

The specific surface areas and pore volumes of the precursor beads were characterized using the nitrogen gas sorption technique, and the typical isotherms are shown in Figure 3. For the precursor beads synthesized with an HDA:Ti molar ratio of 1:1 (PB-1.00HDA-3H_2O), a type II isotherm was observed, indicating its nonporous character.[49] The specific surface area and pore volume were 3.05 m^2/g and 0.008 cm^3/g, respectively, further confirming no porosity. It was found that solution compositions with an HDA:Ti molar ratio of 0.10:1 or higher resulted in similar nonporous precursor beads of low specific surface area and pore volume (see Table 1). By decreasing the HDA:Ti molar ratio to 0.05:1, precursor beads with micropores (less than 2 nm) were obtained, as suggested by the observed type I isotherm (PB-0.05HDA-3H_2O sample in Figure 3).[49] The corresponding specific surface area and pore volume increased to 216 m^2/g and 0.106 cm^3/g, respectively. Further reducing the HDA:Ti molar ratio to 0.02:1 and 0.01:1, precursor beads with much higher specific surface area and larger pore volume were obtained (see PB-0.02HDA-3H_2O and PB-0.01HDA-3H_2O samples in Table 1), and both samples gave the typical type I isotherms, indicating microporous characteristics. In the case of the sample PB-0HDA-3H_2O, prepared in the absence of any structure-directing agent, a type IV isotherm along with two small, but obvious, hysteresis loops at relative pressures of P/P_o = 0.45−0.78 and 0.90−0.98 were observed, indicating the presence of interparticle, nonordered, mesoporosity in this sample.[49] The hysteresis at low P/P_o corresponds to ~4 nm mesopores in the framework of the single precursor bead, while the higher P/P_o hysteresis can be ascribed to the relatively large pores (~81 nm) between the beads. The high specific surface area (422 m^2/g) and large pore volume (0.258 cm^3/g) of this sample confirm this finding.

2. Effect of the H_2O:Ti Molar Ratio. Careful manipulation of the water to titanium ratio is also important for the fabrication of spherical particles and for controlling the size monodispersity and sphere diameter. For example, when insufficient water was added to the system (H_2O:Ti = 1:1), spheres were not formed (see Figure SI-4, SI). Even at a ratio of 2:1, the particles were not quite spherical. The SEM images in Figure 4 show the precursor beads prepared with increasing water to Ti molar ratios of 2:1, 4:1, 6:1, and 10:1. Once a ratio of 3:1 was reached, monodisperse spheres were obtained, and at this ratio the diameter was 1150 ± 40 nm. Increasing the water content further results in a reduction in the diameter of the beads, with a diameter of 730 ± 40 nm at 4:1 and 420 ± 50 nm for 7:1. Above a ratio of 8:1, while the particle size distribution is still narrow, dimers formed. If the samples were prepared at a 10:1 water to Ti ratio, the particle size distribution became more polydisperse (320 ± 80 nm) and more dimers were found. The results demonstrate that the water to Ti molar ratio is an important parameter to control the diameter of the monodisperse beads within the range 3:1 ≤ H_2O:Ti ≤ 8:1. Outside this range, however, the monodispersity, size, and spherical shape were compromised.

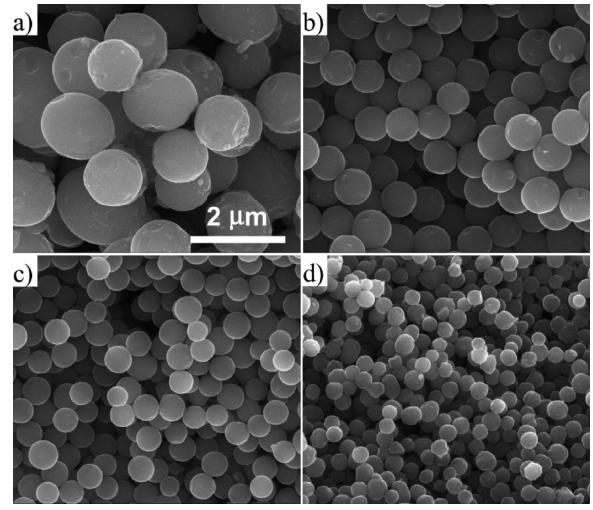

Figure 4. SEM images of the precursor materials synthesized with different H_2O:Ti molar ratios: (a) 2:1, (b) 4:1, (c) 6:1, (d) 10:1. The HDA:Ti molar ratio was kept at 0.5:1 for these samples. These images were taken at the same magnification.

(47) Tanev, P. T.; Chibwe, M.; Pinnavaia, T. J. *Nature* **1994**, *368*, 321.
(48) Tanev, P. T.; Pinnavaia, T. J. *Science* **1995**, *267*, 865.
(49) Lowell, S.; Shields, J. E.; Thomas, M. A.; Thommes, M. *Characterization of Porous Solids and Powders: Surface Area, Pore Size and Density*; Kluwer: London, 2004.

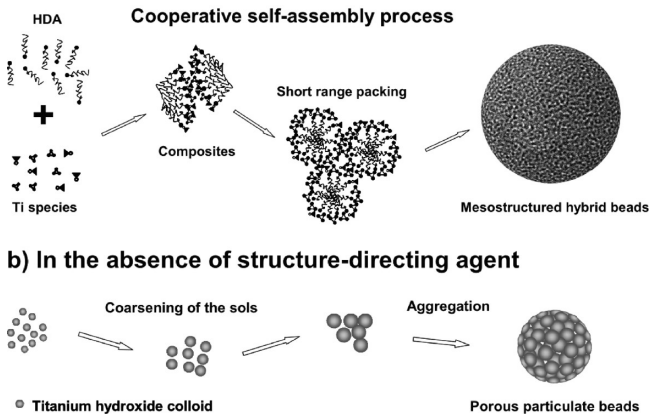

Figure 5. Schematic representation of the formation mechanism of the precursor beads: (a) a cooperative self-assembly process in the presence of HDA as the structure-directing agent and (b) a colloid coarsening and aggregation process in the absence of HDA.

3. Proposed Mechanism for the Formation of Precursor Beads. On the basis of the above results, a formation mechanism of the precursor beads was proposed (see Figure 5) to illustrate the role of HDA as a structure-directing agent affecting the morphology and monodispersity control in the sol−gel synthesis. Monodisperse precursor beads with wormhole-like mesostructures were proposed to form through a cooperative assembly process involving long-chain alkylamine and $Ti(OCH(CH_3)_2)_{4-x}(OH)_x$ species/oligomers.[50] On hydrolysis of TIP, the resultant $Ti(OCH(CH_3)_2)_{4-x}(OH)_x$ species and their oligomers most likely participate in hydrogen-bonding interactions with amino groups of the HDA to form inorganic−organic composites at a molecular level. Such hybrid composites contain hydrophobic long-chain alkyl groups and thus tend to self-organize into rodlike hybrid micelles to reduce the interfacial free energy.[47,48,50] Meanwhile, further hydrolysis and condensation of the titanium species/oligomers associated with the hybrid micelles result in interconnection and short-range packing of the hybrid micelles to form a new liquid condensed phase rich in HDA and titanium oligomers. As the titanium oligomers further polymerize, the condensed phase becomes denser with time, accompanied by the formation of a mesostructured inorganic framework as a result of the gelation transformation, and finally precipitates from the solvent. To minimize the surface free energy, the condensing phase takes a spherical shape as in conventional colloid formation processes.[51,52] Depending on the speed of this phase separation process, the change in optical properties of the solution varies for the different systems: in general, a sudden change from a clear solution to a milky white suspension is observed when a fast phase separation occurs; otherwise, the clear solution first turns into a slightly blue colloidal solution and finally to a milky white suspension when the above phase separation happens gradually with time. Taking into account the induction times (the period of time taken after addition of TIP until the milky white solution forms) observed in this process, the formation of the monodisperse mesostructured precursor beads closely adheres to the proposed mechanism as follows. In Table 1, decreasing the HDA:Ti molar ratio from 1:1 to 0.33:1, the induction time was short and varied only slightly, indicating a very rapid phase separation process, and monodisperse precursor beads form in these cases (Figure 1a). Further decreasing the HDA:Ti molar ratio to 0.25:1, the induction time nearly doubled, indicating a delayed phase separation process, and this gave rise to the formation of dimers along with the monodisperse precursor beads (Figure 1c,d). More dimer particles were produced when the phase separation process was further delayed (31 ± 2 s for sample PB-0.10HDA-$3H_2O$). In the case of the PB-0.05HDA-$3H_2O$ sample, the induction time was almost 10 times longer than that of sample PB-1.00HDA-$3H_2O$, suggesting a considerably prolonged phase separation process was involved, and polydisperse precursor beads were obtained (Figure 1g). It is believed that lipophilic interactions between the long-chain alkyl groups of the inorganic−organic composites act as the driving force to initialize the self-assembly process of the hydrolyzed $Ti(OCH(CH_3)_2)_{4-x}(OH)_x$ species/oligomers to produce monodisperse precursor beads in the sol−gel synthesis.[48,50,53] A higher HDA:Ti molar ratio (over 0.25:1) gives rise to a stronger lipophilic interaction and therefore leads to the formation of monodisperse precursor beads as a result of the enhanced driving force for self-assembly, associated with a quicker phase separation process.

For precursor beads prepared in the absence of HDA, the hydrophilicity of the hydrolyzed titanium species/oligomers was not altered by any organic structure-directing agents, and the formation of polydisperse spherical particles is proposed to

Table 2. Physical Properties of the Calcined Mesoporous Titania Beads[a]

sample name	diameter (nm)	S_{BET} (m^2/g)	PD (nm)	V_{sp} (cm^3/g)
TiO_2-1.00HDA-$3H_2O$-0M	830 ± 40	112	13.8	0.302
TiO_2-0.50HDA-$3H_2O$-0M		116	13.9	0.322
TiO_2-0.33HDA-$3H_2O$-0M		108	14.0	0.333
TiO_2-1.00HDA-$3H_2O$-0.22M		102	18.0	0.385
TiO_2-0.50HDA-$3H_2O$-0.22M		101	17.9	0.413
TiO_2-0.33HDA-$3H_2O$-0.22M		94.2	18.1	0.387
TiO_2-1.00HDA-$3H_2O$-0.45M		90.7	23.1	0.401
TiO_2-0.50HDA-$3H_2O$-0.45M		90.9	22.7	0.437
TiO_2-0.33HDA-$3H_2O$-0.45M		89.1	22.6	0.408
PB-1.00HDA-$3H_2O$-calcined		3.60	na	0.011
PB-0.50HDA-$3H_2O$-calcined		3.52	na	0.010
PB-0.33HDA-$3H_2O$-calcined		3.01	na	0.009
TiO_2-1.00HDA-$4H_2O$-0M	550 ± 50	117	14.2	0.351
TiO_2-0.50HDA-$4H_2O$-0M		120	13.8	0.348
TiO_2-1.00HDA-$4H_2O$-0.22M		102	18.3	0.433
TiO_2-0.50HDA-$4H_2O$-0.22M		102	17.8	0.429
TiO_2-1.00HDA-$4H_2O$-0.45M		92.0	23.3	0.428
TiO_2-0.50HDA-$4H_2O$-0.45M		91.1	23.4	0.428
PB-0.50HDA-$4H_2O$-calcined		5.02	na	0.016
TiO_2-1.00HDA-$7H_2O$-0M	320 ± 50	111	13.8	0.316
TiO_2-0.50HDA-$7H_2O$-0M		106	14.1	0.342
TiO_2-1.00HDA-$7H_2O$-0.22M		94.9	17.9	0.363
TiO_2-0.50HDA-$7H_2O$-0.22M		93.4	17.8	0.377
TiO_2-0.50HDA-$7H_2O$-0.45M		91.3	23.0	0.395
TiO_2-1.00HDA-$7H_2O$-0.45M		90.3	22.8	0.413
PB-1.00HDA-$7H_2O$-calcined		5.83	na	0.025

[a] S_{BET} = BET specific surface area obtained from N_2 adsorption data in the P/P_o range from 0.05 to 0.20. PD = pore diameter determined by using the BJH model from the N_2 adsorption data. V_{sp} = single-point pore volume calculated from the adsorption isotherm at $P/P_o = 0.98$. "na" indicates the pore diameter could not be determined from N_2 sorption data.

(50) Monnier, A.; Schüth, F.; Huo, Q.; Kumar, D.; Margolese, D.; Maxwell, R. S.; Stucky, G. D.; Krishnamurty, M.; Petroff, P.; Firouzi, A.; Janicke, M.; Chmelka, B. F. *Science* **1993**, *261*, 1299.
(51) Yu, C. Z.; Fan, J.; Tian, B. Z.; Zhao, D. Y. *Chem. Mater.* **2004**, *16*, 889.
(52) Stöber, W.; Fink, A.; Bohn, E. *J. Colloid Interface Sci.* **1968**, *26*, 62.
(53) Arabatzis, I. M.; Falaras, P. *Nano Lett.* **2003**, *3*, 249.

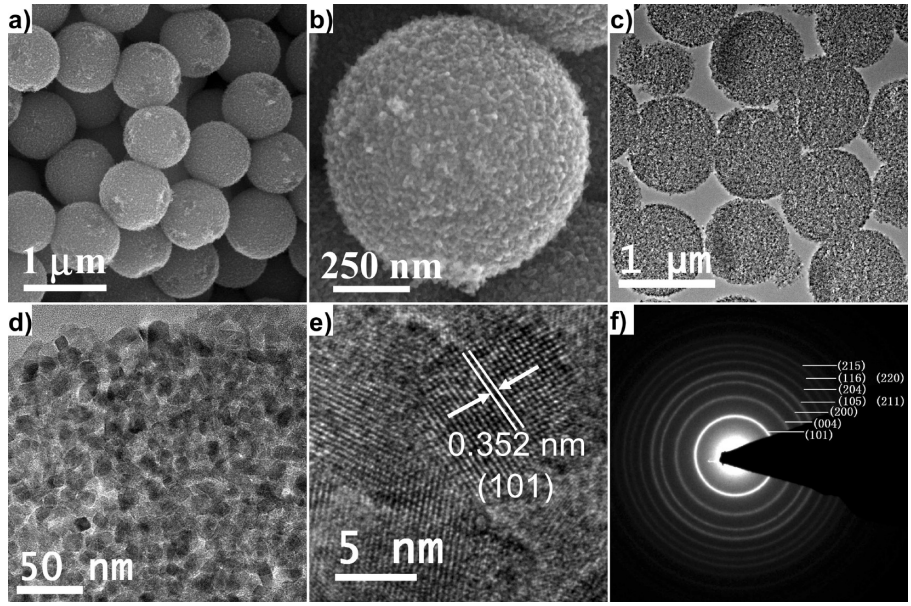

Figure 6. Mesoporous TiO_2 beads obtained after solvothermal treatment and calcination: (a, b) SEM images of the spheres, (c, d) TEM images of the ultramicrotomed sample, (e) HRTEM image of the anatase crystal, (f) SAED pattern. The sample was prepared with an HDA:H_2O:Ti molar ratio of 0.5:3:1 during precursor bead formation and in the absence of ammonia during the solvothermal process.

follow well-documented colloid coarsening and aggregation processes.[54−56] This mechanism is supported by the following results: (1) such beads (PB-0HDA-3H_2O) possess abundant interparticle micro/mesoporosity derived from the aggregated sol particles as suggested by their high specific surface area (422 m^2/g) and large pore volume (0.258 cm^3/g); (2) the beads possess granular features on the outer surfaces, indicating aggregation of tiny sol particles as revealed by the high-resolution SEM image (Figure 1i), and this result is further supported by the existence of ∼5 nm crystalline particles within the amorphous matrix as shown in the HRTEM image (Figure 2f).

Mesoporous Anatase Titania Beads. The amorphous precursor beads can crystallize into anatase titania materials after a direct calcination treatment at 500 °C for 2 h in air; however, the resultant titania beads possess very low specific surface area and pore volume (calcined samples in Table 2). However, for the titania beads that underwent a solvothermal treatment followed by calcination at 500 °C in air, specific surface areas as high as ∼110 m^2/g can be achieved in the absence of ammonia during solvothermal treatment (see TiO_2-*x*HDA-*y*H_2O-0M samples in Table 2). The samples possess a narrow pore size distribution centered at 14.0 ± 0.2 nm regardless of the bead diameter. Adding ammonia at a concentration of 0.22 M in the solvothermal process results in an obvious increase in pore size from 14 to 18 nm along with a slight decrease in specific surface area. Increasing the ammonia concentration to 0.45 M, the pore size of the mesoporous titania beads was enlarged to 23 nm, while the specific surface area was ∼90 m^2/g.

The beads retain their monodispersity (Figure 6a) with some shrinkage (diameter of 830 ± 40 nm) compared with the original

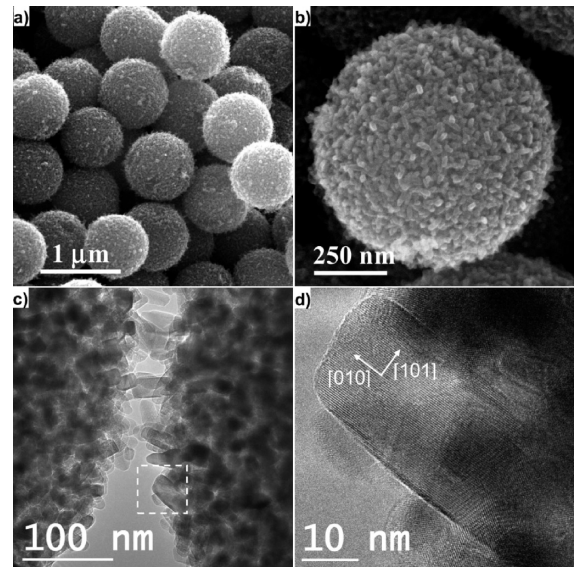

Figure 7. Mesoporous TiO_2 beads obtained after solvothermal treatment and calcination: (a, b) SEM images of the spheres, (c) TEM images of the ultramicrotomed sample, (d) HRTEM image of the elongated anatase crystal. The sample was prepared with an HDA:H_2O:Ti molar ratio of 0.5:3:1 during precursor bead formation and with 0.45 M ammonia during the solvothermal process.

precursor beads and are composed of nanoparticles as seen by the rough surface of the beads in the SEM images and the particles in the TEM images (Figure 6b−d). However, the wormhole-like mesostructure in the precursor spheres is not carried through to the final beads as indicated by TEM images (Figure 6d) and featureless SAXRD patterns (see Figure SI-5, SI). Disordered mesopores (intercrystalline pores) are abundant throughout the bead structure (Figure 6c,d). At higher magnifications the individual crystals (14.5 ± 0.5 nm) of anatase TiO_2 are clearly observed. The HRTEM image allows the resolution of lattice fringes of the crystals to be correlated to the (101)

(54) Vanblaaderen, A.; Vangeest, J.; Vrij, A. *J. Colloid Interface Sci.* **1992**, *154*, 481.
(55) Hunter, R. J. *Foundations of Colloid Science*, 2nd ed.; Oxford University Press: New York, 2001.
(56) Widoniak, J.; Eiden-Assmann, S.; Maret, G. *Eur. J. Inorg. Chem.* **2005**, 3149.

planes of the anatase titania (Figure 6e). The distinct SAED pattern also confirms the crystalline anatase phase of the sample (Figure 6f).

When ammonia was added to the solvent for solvothermal treatment, the crystal growth was altered, resulting in elongated TiO_2 crystals and consequently variation in the pore size in the final spheres. From gas sorption data the pore size increased from 14 to 18 and 23 nm as the ammonia concentration increased from 0 to 0.22 and 0.45 M.[36] The monodispersity and sphere diameter were not affected by the presence of ammonia (Figure 7a,b). TEM images of the ultramicrotomed beads along with an HRTEM image of an anatase crystal show elongated TiO_2 grains when 0.45 M ammonia solution was used during solvothermal treatment (Figure 7c,d). The anatase crystal growth occurs along the [010] direction, increasing the abundance of the (101) plane.

Summary

We have demonstrated the possibility of producing mesoporous titania materials with integrated features, including high specific surface area, large pore size, high crystallinity, and well-defined morphologies, via a combined sol−gel and solvothermal process in the presence of hexadecylamine as a structure-directing agent. By adjusting the HDA concentration and the H_2O content during the sol−gel synthesis, the morphology, monodispersity, and diameter (from ∼320 to 1150 nm) of the resultant titania beads can be tuned via a cooperative self-assembly process. Varying the ammonia concentration in a mild solvothermal process gives rise to mesoporous anatase titania beads having controllable crystallite size, specific surface area (from 89 to 120 m^2/g), and pore size distribution (from 14 to 23 nm). The resultant mesoporous titania materials are expected to have potential applications in areas of energy conversion and environmental cleanup. The simplicity and reproducibility of this synthetic approach is expected to extend to the production of other versatile mesoporous metal oxide bead materials.

Acknowledgment. This research was financially supported by an Australian Research Council Discovery Project. Dr. Simon Crawford is thanked for ultramicrotoming samples in preparation for TEM characterization. The Electron Microscopy Unit of the Bio21 Institute at The University of Melbourne is acknowledged for electron microscopy access.

Supporting Information Available: Small/wide-angle XRD patterns and HRTEM and SEM images for both the amorphous precursor beads and mesoporous anatase titania materials. This material is available free of charge via the Internet at http://pubs.acs.org.

JA100040P

Supporting Information

Synthesis of monodisperse mesoporous titania beads with controllable diameter, high surface areas and variable pore diameters (14 - 23 nm)

Dehong Chen[1], Lu Cao[1], Fuzhi Huang[3], Paolo Imperia[4], Yi-Bing Cheng[3*], Rachel A. Caruso[1,2,*]

[1]PFPC, School of Chemistry, The University of Melbourne, Melbourne, Victoria, 3010 (Australia)

[2]CSIRO Materials Science and Engineering, Private Bag 33, Clayton South, Victoria, 3169 (Australia)

[3]Department of Materials Engineering, Monash University, Melbourne, Victoria, 3800 (Australia)

[4]The Bragg Institute and Institute of Materials Engineering, ANSTO, Lucas Heights, New South Wales, 2234 (Australia)

Prof. Yi-Bing Cheng email: yibing.cheng@eng.monash.edu.au
Dr. Rachel A. Caruso email: rcaruso@unimelb.edu.au

Supporting Information

Figure SI-1. Small angle XRD patterns of the precursor beads synthesized with an HDA:Ti molar ratio of 1:1 and without the HDA structure-directing agent. The H_2O:Ti molar ratio was 3:1 for these samples.

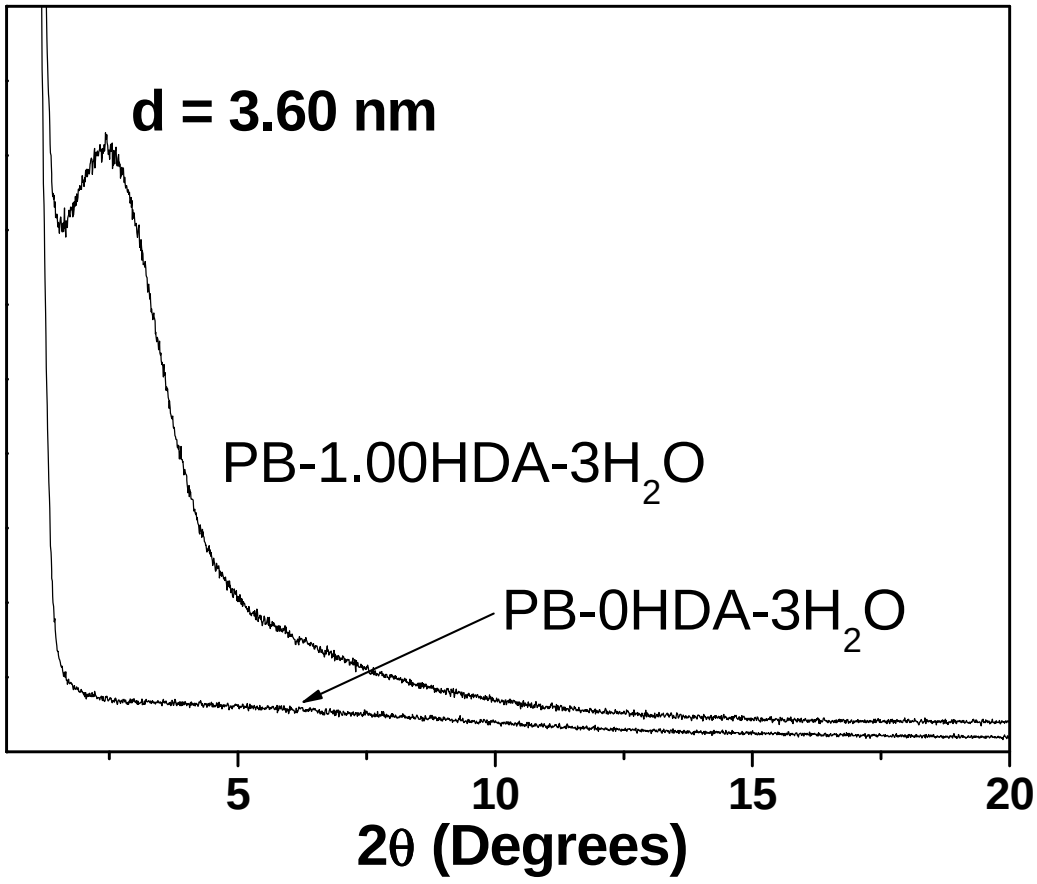

Supporting Information

Figure SI-2. Wide angle XRD of the precursor beads prepared with varying HDA/Ti molar ratio. Regardless of HDA concentration, the featureless wide angle XRD patterns revealed that these precursor beads were amorphous.

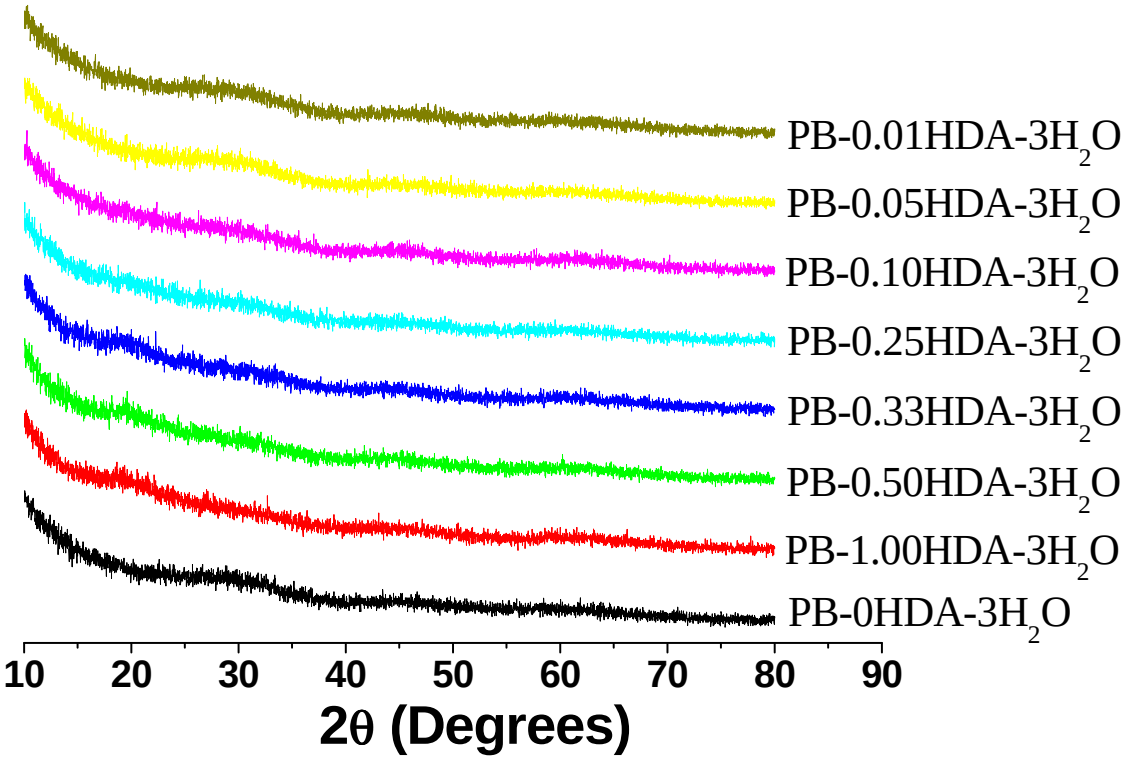

Supporting Information

Figure SI-3 HRTEM image of the crystalline nanoparticles shown in Fig. 2f. A detailed analysis along the white line suggested a lattice fringe of 0.3524 nm (inset), which can be indexed to the (101) planes of the anatase titania (0.352 nm for anatase (101) planes, JCPDS card No. 21-1272).

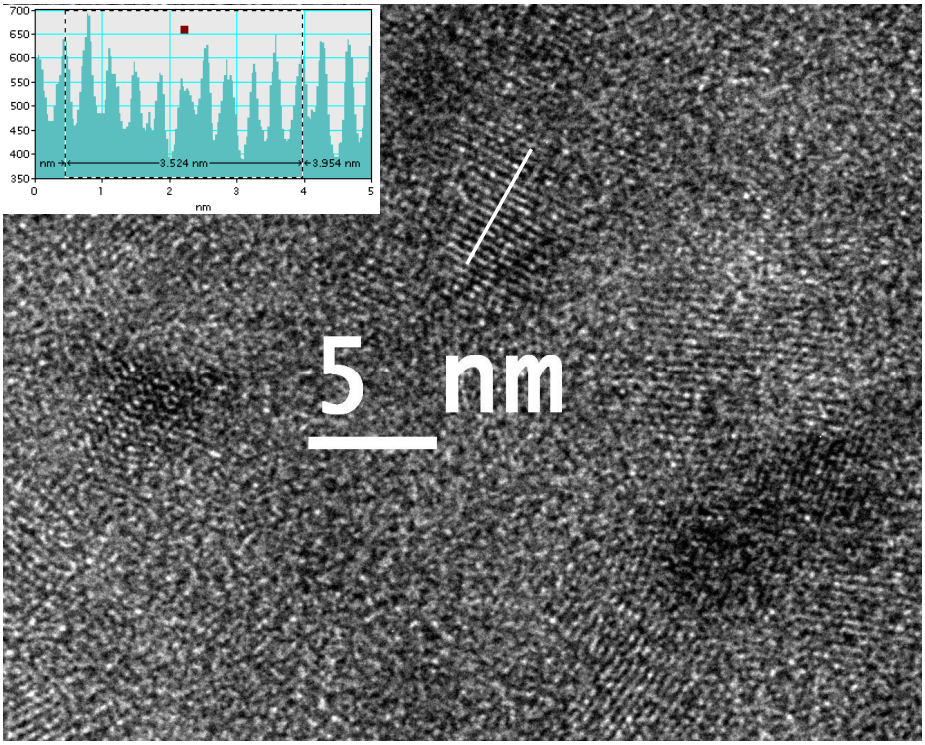

Supporting Information

Figure SI-4 SEM images of the precursor materials synthesized with different H_2O:Ti molar ratios: a) 1:1; b) 3:1; c) 5:1; and d) 8:1. The HDA:Ti molar ratio was kept at 0.5:1 for these samples. All the images were taken at the same magnification.

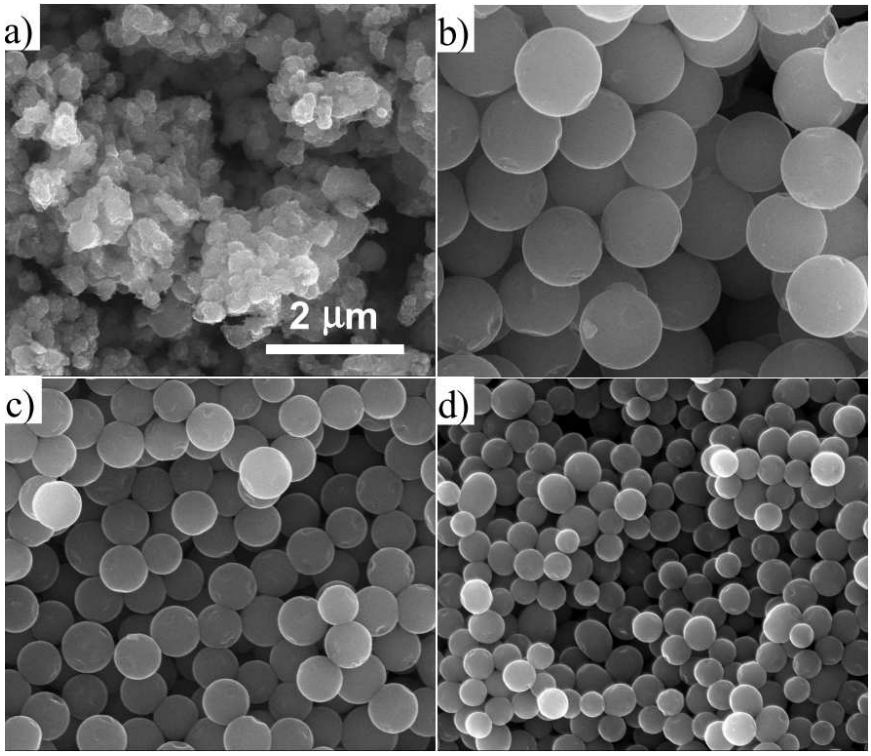

Figure SI-5. Small angle XRD patterns of the solvothermally treated (black curve) and calcined mesoporous titania beads (red curve). The featureless SAXRD patterns indicate the absence of any mesostructures.